Distribution Agreement

In presenting this thesis as a partial fulfillment of the requirements for a degree from Emory University, I hereby grant to Emory University and its agents the non-exclusive license to archive, make accessible, and display my thesis in whole or in part in all forms of media, now or hereafter now, including display on the World Wide Web. I understand that I may select some access restrictions as part of the online submission of this thesis. I retain all ownership rights to the copyright of the thesis. I also retain the right to use in future works (such as articles or books) all or part of this thesis.

Mark Kravitz April 11, 2017

Neuroanatomical and electrophysiological characteristics of dorsal column stimulation in the adult mouse

by

Mark Kravitz

Shawn Hochman, PhD
Adviser

Department of Neuroscience and Behavioral Biology

Shawn Hochman, PhD
Adviser

Francisco Alvarez, PhD
Committee Member

Astrid Prinz, PhD
Committee Member

2017

Neuroanatomical and electrophysiological characteristics of dorsal column stimulation in the adult mouse

By

Mark Kravitz

Shawn Hochman, PhD
Adviser

An abstract of
a thesis submitted to the Faculty of Emory College of Arts and Sciences
of Emory University in partial fulfillment
of the requirements of the degree of
Bachelor of Sciences with Honors

Department of Neuroscience and Behavioral Biology

2017

Abstract
Neuroanatomical and electrophysiological characteristics of dorsal column stimulation in the adult mouse
By Mark Kravitz

In this study, I present anatomical and physiological findings related to the composition of primary afferents in the adult mouse dorsal column. Analyzing electron microscope images, I manually counted unmyelinated and myelinated axons, calculated mean axon diameters, and characterized distribution of these fibers throughout the dorsal column. My findings demonstrate the presence of both myelinated and unmyelinated fibers with diameters consistent with Aβ, Aδ, and C fibers. Using *in vitro* electrophysiology techniques in four adult mouse spinal cords, I recorded and analyzed the recruitment of afferent fiber populations in the L6 and S1 dorsal roots during medial dorsal column stimulation at the T10 and L5 segmental levels in the presence of high and low concentrations of calcium. My findings demonstrate the recruitment of Aβ, Aδ, and C fibers as well as calcium-dependent, synaptically mediated activity. This study is significant in that it is one of the few of its kind to be done in adult mouse whole spinal cord preparations, an important model of the mammalian central nervous system. The findings presented in this study add to an understudied field of basic neuroanatomy and electrophysiology of the mechanism underlying dorsal column stimulation, a neurostimulatory therapy currently used clinically for chronic pain, but with potential uses in other neurological disorders.

Neuroanatomical and electrophysiological characteristics of dorsal column stimulation in the adult mouse

By

Mark Kravitz

Shawn Hochman, PhD
Adviser

An abstract of
a thesis submitted to the Faculty of Emory College of Arts and Sciences
of Emory University in partial fulfillment
of the requirements of the degree of
Bachelor of Sciences with Honors

Department of Neuroscience and Behavioral Biology

2017

Acknowledgements

I would like to thank Dr. Shawn Hochman for his continued guidance, support, and teachings as my advisor for the past two years and inspiring me to pursue a career in biomedical research. I would like to thank Dr. Francisco Alvarez and Dr. Astrid Prinz for their assistance, knowledge, and time spent as valued members of my thesis committee. I would like to thank Shaquia Idlett for serving as my mentor for the past two years, teaching me everything I know about the spinal cord. I would like to thank the rest of the Hochman lab – Michael Sawchuk, Michael McKinnon, Mallika Halder, and Makalele Gorsich – for their support and friendship, and for welcoming me into their lab with open arms. Finally, I would like to thank Hong Yi and the Robert P. Akparian Integrated Electron Microscopy Core at Emory University for their assistance in my neuroanatomy experiments.

Table of Contents

Introduction and Background……1

Objectives……7

Materials and Methods……10

Results……16

Discussion……19

Conclusion……22

References……23

Tables and Figures……28

Introduction & Background

Before discussing the objectives, methods, and results of my project, I first provide some basic information regarding spinal cord anatomy and physiology. I then go into a detailed description of a white matter region of the spinal cord known as the dorsal (posterior) column. Following that description, I discuss the history and uses of spinal cord stimulation (SCS), a neurostimulation method that targets the dorsal column. Finally, I conclude with a discussion of spinal cord injury, specifically focusing on deficits in bladder function and the potential of SCS to be used to restore bladder function in SCI paralyzed individuals.

Spinal Cord Anatomy and Physiology

The spinal cord is a bundle of nervous tissue encased by the vertebral column and extends from the brain stem to the second lumbar vertebrae, relaying motor, sensory, and autonomic information between the central and peripheral nervous systems (Fig 1). Neural signals are transmitted by two functionally and anatomically distinct regions of the spinal cord. The ventral, or anterior, region of the spinal cord relays descending motor commands to muscles in the periphery while the dorsal, or posterior, region transmits ascending sensory information (Gianino et al., 1996). Longitudinally, the human spinal cord is divided into thirty-one segments: eight cervical, twelve thoracic, five lumbar, five sacral, and one coccygeal. Each spinal segment has a pair of ventral roots, which contain efferent motor neurons, and a pair of dorsal roots, which contain afferent sensory neurons. Dorsal root neurons have cell bodies located in dorsal root ganglion, and relay

touch, proprioception, temperature, and pain signals from the periphery to brain. Each pair of dorsal roots corresponds to a region of skin, known as a dermatome, which it innervates. The cross-sectional organization is essentially uniform across all levels consisting of a butterfly shaped region of grey matter (neuronal cell bodies and interneurons) surrounded by white matter (axonal ascending and descending tracts). The grey matter is organized into ten functionally specific laminae and the white matter is organized in several functionally specific tracts (Rexed 1954), one of which being the dorsal column.

Primary Afferents of the Dorsal Column

One tract that has gained attention in clinical and basic research disciplines is the dorsal column. The dorsal column consists of axons located in the posterior white matter of the spinal cord. These axons project to dorsal column nuclei of the medulla and terminate on second order neurons, which project to the thalamus and ultimately the postcentral gyrus of the cerebral cortex. It is believed that the dorsal column relays sensory information to the cortex related to touch, temperature, and proprioception. Dorsal column primary afferents enter the spinal cord from the periphery through dorsal roots, project medially into the dorsal column, and bifurcate branches rostrally and caudally (Willis & Coggeshall, 2004). Only a fraction of these fibers that enter the dorsal column ascend all way to the medulla (Glees & Soler, 1951). Based on their distance traveled, the fibers fall into one of three categories: 1) afferents that terminate within one or two spinal segments (short system), afferents that project rostrally 4-12 segments before terminating

(intermediate system), and afferents that project all the way to the medulla (long system) (Horch et al., 1976). Axons in the long system migrate more medially as they ascend the cord, meaning that the medial region of the dorsal column contains a larger proportion of axons that entered the cord from distant roots than the lateral region (Horch et al., 1976).

The composition of these primary afferents has been the subject of debate between researchers. *In vitro* electrophysiology experiments have demonstrated that dorsal column stimulation recruits fibers with conduction velocities consistent with Aβ and Aδ afferents (Baba et al., 1994; Shimizu et al., 1995; Okamoto et al., 2000). Imaging studies of the dorsal column of rats in the 1980s, however, revealed the presence of both myelinated axons with average diameters of 1.06 +/- 0.57 μm and unmyelinated C fibers with average diameters of 0.3 +/- 0.1 μm (McNeill et al., 1988; See Table 1). The relationship between axon diameter and conduction velocity is a positive correlation, meaning that the small diameter axons of C fibers are the slowest conducting fibers and conduction velocity is the greatest in the large, thickly myelinated motor neurons (Hursh, 1939). Dorsal column stimulation studies of primary afferent conduction velocities in mammals have supported this relationship, as the larger Aβ fibers conduct at velocities greater than 10 m/s, smaller diameter Aδ fibers conduct at velocities between 1 and 10 m/s, and the smallest C fibers conduct at less that 1 m/s (Harper & Lawson, 1985; Pinto et al., 2008; See Table 1). Despite these findings, modern computational models of the dorsal column used in the development of spinal cord stimulators have ignored the

presence of these C fibers and have even used ion channel dynamic properties related to motor neurons instead of primary afferents (Holsheimer 1998).

History of Spinal Cord Stimulation (SCS)

SCS was developed following Melzack and Wall's 1965 publication describing the "gate control theory" of pain. This theory proposed that inhibitory interneurons in the dorsal grey matter, known as the dorsal horn, act as a gate for signaling pain from the periphery to the brain (Melzack and Wall, 1965). The idea behind SCS proposed that stimulation of the dorsal column activates large diameter fibers which propagate antidromically and act on these interneurons to effectively "close the gate", blocking the transmission of painful information by small diameter fibers, thus reducing the perception of pain. The theory has been amended as many concerns arose from its simplicity (Braz et al., 2014); however it remains the backbone of understanding pain transmission in the spinal cord.

SCS was first used to treat chronic pain in the late 1960s (Shealy et al., 1967). Recently, the efficacy is described by a 50/50 rule: 50% of the patients implanted with a trial stimulator report at least 50% pain relief and go on to receive a permanent implant (Kumar et al., 2007). Currently, studies are investigating the potential of using SCS to treat conditions beyond just chronic pain such as Parkinson's disease (Fuentes et al., 2009), partial and complete paralysis (Harkema et al., 2011), and bladder, bowel, and sexual dysfunction (Meglio et al., 1980).

Despite clinical successes, animal models, and preclinical investigations, the mechanisms leading to SCS-mediated pain relief remain unclear. While the "gate

control theory" provides the potential framework for the underlying mechanism of action, studies have since demonstrated more complexity than the "gate control theory" model encompasses, such as C fiber projections in the dorsal column (Braz et al., 2014). The lack of a precise understanding of the circuitry being modulated may explain sustained low success rates (North et al., 1993; Cameron, 2004). Furthermore, determining the mechanism of action may open doors to potential future uses of SCS, such as treating bowel and bladder dysfunction following a SCI. In order to understand how SCS works, it is imperative to study the anatomy and circuitry recruited with dorsal column stimulation

Spinal Cord Injury Etiology, Pathology, and Symptomology

Spinal cord injury (SCI) describes the wide range of pathologies associated with damage to the spinal cord. Approximately 240,000-337,000 people in the U.S. are living with a SCI, with about 12,500 new cases per year (National Spinal Cord Injury Statistics Center, 2014). Deficits in voluntary motor function are a notable complication following SCI. Depending upon the location and severity of neural damage, an individual may be partially or completely paralyzed below the level of injury. Less noted, however, are the sensory and autonomic deficits caused by SCI. About 60-70% of patients with SCI report having chronic pain and may present other sensory changes, such as hypersensitivity, paresthesia, or hypoesthesia (Dijkers et al., 2009). Another major complaint of patients with SCI is dysfunction of their autonomic nervous system, such as the loss of bowel and bladder control. In fact, the number one reason patients with SCI go to the emergency room is infection

due to the inability to voluntarily void their bladder (Anderson 2004). In a survey of patients with SCI, when asked what function they would most prefer to regain, the majority said "bowel/bladder function" (Anderson 2004). While many studies seek to understand the motor and sensory deficits associated with SCI, far fewer address the implications upon bladder and bowel function, despite its clinical relevance.

Attempts have been made over the last two hundred years to alleviate bladder dysfunction through neuromodulation. The first study was in the late 19th century by Danish surgeon Dr. Mathias Saxtorph using intravesical stimulation to treat urinary retention (Madersbacher 1990). Then, in the 1950s, W. H. Boyce developed the implantable bladder wall stimulator (Boyce et al., 1965). These methods were generally unsuccessful. In the 1960s, several studies focused on developing pelvic and sacral anterior root stimulators, which has since been the model of electrical stimulation for urinary incontinence (Bors & Comarr, 1971). Animal models have demonstrated that SCS is more effective at inducing bladder voiding in SCI paralyzed rats than bladder wall or pelvic nerve stimulation (Gad et al., 2014). Furthermore, the surgery to implant a spinal cord stimulator is less invasive and carries fewer risks than the surgery required for sacral anterior root stimulation (Rijkhoff et al., 1997). It is known that the bladder is innervated by both Aδ and C afferents (Keast & De Groat, 1992). Studies have demonstrated that SCI induces hypersensitivity of these C fibers, leading to bladder dysfunction and that stimulation of these fibers may inhibit their activity, restoring voluntary bladder control (Hong et al., 2008). Therefore, SCS may provide a more effective, less risky alternative treatment for bladder dysfunction in paralyzed individuals.

Objectives

In order to investigate the mechanisms underlying SCS in relation to its potential use to restore bladder function following spinal cord injury, I took a two-tiered approach: neuroanatomical and electrophysiological. The neuroanatomy study focuses on the characteristics of axons located in the T10 dorsal column of the adult mouse. T10 was chosen because it is a level commonly used in clinical applications of SCS (Wheeler, 2015). The electrophysiology study focuses on the afferent fiber recruitment characteristics of the L6 and S1 dorsal roots during dorsal column stimulation. L6 and S1 were targeted because these roots contain primary afferents related to bladder sensory information in rats (Birder et al., 1999) and mice (Jansenn et al., 2016).

Neuroanatomical characteristics of T10 adult mouse dorsal column

The neuroanatomy of the mammalian dorsal column has been well established using imagining studies in rats (Gulley, 1973), cats (Hand, 1966), and nonhuman primates (Qi and Kaas, 2006). However, few studies have investigated the neuroanatomical characteristics of mice. The mouse will undoubtedly become an important model for dorsal column stimulation studies as it allows for genetic manipulation application of molecular techniques that allow for elegant analysis of neural circuitry. Without sufficient anatomical evidence to support physiological findings, important considerations may be overlooked when developing future models. For example, many of the computational models for SCS ignore the influence of stimulation on unmyelinated fibers in the dorsal column, despite ample

anatomical evidence (Holsheimer 1998). This is likely due to differing objectives between engineers and neuroanatomists. Engineers aim to develop an elegant computational model that ultimately functions efficiently, whereas neuroanatomists try to demonstrate the intricate complexities of the system. Approaching the neuroanatomy of the mouse dorsal column with the goal of understanding SCS will hopefully bridge this gap and provide important structural evidence for future SCS studies in mice. Therefore, I propose that analyzing the axon fiber composition and mean axon diameters of fibers in the T10 mouse dorsal column will demonstrate the presence and important anatomical characteristics of both myelinated and unmyelinated fibers at the location of SCS.

Electrophysiological characteristics of lumbar and sacral root afferents recruited during dorsal column stimulation

In vivo and *in vitro* studies have suggested the potential use of SCS to modulate circuitry involved in bladder voiding in paralyzed animal models (Gad et al., 2014; Abud et al., 2015). While these studies have demonstrated the ability to initiate micturition using SCS, the underlying mechanism of how the implicated circuitry is modulated is unknown. Understanding what afferent fiber axon populations are recruited and their electrophysiological characteristics during dorsal column stimulation may inform future studies into this mechanism and perhaps lead to clinical investigations for the use of SCS in bladder dysfunction. In mice, the afferent fibers associated with bladder sensory information are Aδ and C afferents (Keast & De Groat, 1992) located in the L6 and S1 dorsal roots (Jansenn et

al., 2016). Based on anatomical and physiological studies of the dorsal column, long system afferent fibers project from dorsal roots and ascend the dorsal column (Horch et al., 1976). Therefore, I propose that stimulation of the dorsal column at T10 and L5 will recruit Aβ, Aδ, and C fiber populations, determined by their conduction velocity, in the L6 and S1 dorsal roots.

Materials and Methods

Neuroanatomy Methods

Imaging procedure

Cross-section slices of T10 were taken from two adult mice and fixed first with 2.5% glutaraldehyde solution. The tissue was then fixed using a 1% osmium tetroxide solution and stained with 5% uranyl acetate and 2% lead citrate. Images of these slices were taken using a JEOL JEM-1400 Transmission Electron Microscope at 16000x magnification at the Robert P. Akparian Integrated Electron Microscopy Core at Emory University. These images were first processed using IMOD version 4.9 software. The images were cropped into 5.13 μm x 5.13 μm images for ease of analysis. The cross-sections were carefully chosen to exclude areas of the corticospinal and Lissauer's tract to ensure analysis of only dorsal column neurons. The boundaries were determined by previous work demonstrating that Lissauer's tract contains a higher proportion of unmyelinated and small diameter myelinated axons than the dorsal column (Chung et al., 1979) and studies revealing a more uniform distribution of only small diameter myelinated axons in the corticospinal tract (Watson & Harrison, 2012). Furthermore, both of these neighboring tracts lack any large diameter myelinated axons. Based on these morphological guidelines, the boundaries of the dorsal column were set.

Analysis of axonal characteristics

The 5.13 μm x 5.13 μm images were then analyzed using ImageJ 1.49 version software. Analysis of each image included manual counts of myelinated and unmyelinated fibers, calculations of mean axon diameters of the myelinated fibers, and, when possible, mean axon diameters of the unmyelinated fibers. Total myelinated and unmyelinated fiber counts were determined for the dorsal column, and the distribution of myelinated and unmyelinated fibers in various regions in the dorsal column were also determined (Fig 5b-c). To determine the mean axon diameter of the myelinated fibers, I used ImageJ particle detection and averaged two ferret diameters. Due to the contrast of the images, the software did not always identify the unmyelinated fibers so the mean axon diameter was estimated by hand using the average of two perpendicular diameters.

The distributions of myelinated mean axon diameters were then presented as percentages of the total number of myelinated fibers. The statistical analysis involved determining the mean and standard deviation of these percentages from the two animals analyzed (Fig 5d).

Electrophysiology Methods

Cord Preparation

Four adult C57/B6 mice (P60 or older) were deeply anesthetized with a 20% ketamine-12.5% xylazine mix by intraperitoneal injection, following light anesthetization in an isoflurane chamber. Fur and skin were removed from a section over the vertebral column, allowing for quick access to the upper thoracic through

lower sacral vertebrate. To lower the body temperature, the dorsal sides of the animals were placed in an ice bath for 2-3 minutes. The animals were decapitated, the ribs and vertebral column were excised from the animal, and then placed in ice cold, oxygenated high Mg^{2+}, low Ca^{2+} artificial cerebral spinal fluid (aCSF), [NaCl 128 mM, KCl 1.9 mM, $MgSO_4$ 13.3 mM, $CaCl_2$ 1.1 mM, KH2PO4 1.2 mM, Glucose- 10 mM, NaHCO3 26 mM]; while a rapid (~5 min) vertebrectomy and spinal cord isolation was performed. The isolated cord was placed in a mesh-bottomed chamber, floating within a glass dish containing room temperature, oxygenated aCSF, [NaCl 128 mM, KCl 1.9 mM, $MgSO_4$ 1.3 mM, $CaCl_2$ 2.4 mM, KH_2PO_4 1.2 mM, Glucose 10 mM, $NaHCO_3$ 26 mM]; with a stir bar for 1 hour. After the 1 hour resting period, the spinal cord was pinned dorsal side up in an Sylgard-lined recording chamber while oxygenated, room temperature aCSF was superfused at a ~40ml/minute.

Electrode Placement

The stimulation and recording set-ups are summarized in figure 2. Three glass suction electrodes were used in these experiments. Two of the electrodes served as recording electrodes and were attached to distal and proximal ends of the dorsal root being recorded (Fig 2b). The roots recorded from in the experiments were L6 and S1, the roots known to contain afferents involved in bladder and bowel sensory information in mice. The other electrode was the stimulating electrode and was placed at the midline of the dorsal column. The stimulating electrode was positioned to contact the surface of the dorsal column but no suction was applied and compression was minimal. The dorsal column was stimulated at two specific

segmental levels: T10 and L5. These levels were chosen because T10 is the location at which current SCS electrodes target and was the region analyzed in the neuroanatomy experiments and L5 was selected to identify any differences in afferent recruitment due to its proximity to the recording electrodes and recruitment of short system afferents. The internal diameters of the recording electrodes were between 100-125 μm, and the internal diameter of the dorsal column stimulating electrode was 83 μm.

Stimulating and Recording Parameters

The dorsal column was stimulated at 50, 100, 200, and 500 μA for 200 and 500 μs. These parameters were selected because a) in modeling data, intensities of 50, 100, and 200 μA for durations of 200 and 500 μs have been used to generate clinically analogous electric fields in the adult mouse spinal cord (study in preparation for publication) and b) they are known to recruit afferent fiber populations at room temperature (Pinto et al., 2008). Extracellular recordings of the L6 and S1 dorsal roots were taken a using differential amplifier, gain set to 1000x, and high and low pass filters set at 1 Hz and 3 kHz, respectively. For each level stimulated and root recorded, there was stimulation directly on the midline of the dorsal column.

Following all recordings in physiologic aCSF, the aCSF was replaced with high magnesium, low calcium containing aCSF to block synaptic transmission (Shreckengost et al., 2010) and all stimulations were repeated. Following stimulation in the low calcium bath, regular aCSF was returned to the bath and all

experiments were repeated once more. This paradigm allowed for the identification of any calcium-dependent synaptically mediated responses recruited by dorsal column stimulation.

For every stimulation, ten recording sweeps were taken. Baselines of these recordings were adjusted and averages of each trace were determined using pClamp 10 software. Data is shown with the average trace in bold color and raw traces are depicted as light gray (Figs 3 and 6).

Conduction Velocity Determination

The main outcome measure of these experiments was conduction velocity. The electrode set up allows for two different readings of conduction velocity – central and peripheral. For each experiment, the distances between the stimulating electrode, the proximal electrode, and the distal electrode were measured. When stimulating at T10, the distance between the stimulating electrode and proximal electrode ranged from 10-13 mm, and when stimulating at L5, the distance ranged from 4-6 mm, with individual difference between animals. The distance between the two recording electrodes was about 3-4 mm, but varied depending on the length of the root. Using these known distances, central and peripheral conduction velocity can be determined (Fig 3). These conduction velocities were compared to previous studies identifying the conduction velocities of primary afferents at room temperature (Pinto et al., 2008).

Results

Neuroanatomy Results

Characteristics of unmyelinated fibers in the dorsal column

Low magnification electron micrograph images of the dorsal column appear to show populations of myelinated fibers with varying axon diameters (Fig 4b). Higher magnified images (Fig 4c-d) reveal the presence of small, unmyelinated fibers. These fibers are typically found in bundles of about 10-25 unmyelinated fibers. These unmyelinated fibers range from 0.1 – 0.3 μm, but may be as large as 0.5 μm. These characteristics are consistent with C fibers in mouse (Ong & Wehrli, 2010).

Characteristics of myelinated fibers in the dorsal column

Myelinated fibers are abundant in the dorsal column (Fig 4b-f). These fibers range in internal diameter and thickness of myelin (Fig 4f). The mean axon diameters of the myelinated fibers range from 0.3 – 6.0 μm, but the majority (~70%) fall in the range of 0.5 – 1.5 μm (Fig 5d). These fiber diameters are consistent with Aβ and Aδ afferents known to exist in the dorsal column found in other animal models (Almeida et al., 2004; Ong & Wehrli 2011).

Distribution of unmyelinated and myelinated fibers in the dorsal column

Unmyelinated fibers are present throughout the dorsal column, but in different proportions depending on location. In the more medial and ventral regions

of the dorsal column, near the corticospinal tract, there is about a 1:1 ratio of unmyelinated to myelinated fibers (Fig 5b). The myelinated fibers in the medial region are typically smaller in diameter and are densely packed together, about 1 fiber per μm^2 (Fig 4e). In more lateral regions of the dorsal column near the dorsal horn and near the surface of the cord, the ratio of unmyelinated to myelinated fibers increases to about 2:1 (Fig 5c). In these lateral regions, the myelinated fibers are more spread out and tend to be larger in diameter.

Electrophysiology Results

Dorsal column stimulation recruits three populations of primary afferents

In vitro T10 and L5 dorsal column stimulation experiments were performed in four adult mice spinal cords at intensities of 50, 100, 200, and 500 μA with pulse durations of 200 and 500 μs. Stimulation of the dorsal column at T10 and L5 activated afferent fiber population recorded from the L6 and S1 roots. At lower intensity stimulations, fibers with a conduction velocity ranging from 10.0 – 30.0 m/s were recruited, consistent with activation of Aβ fibers at room temperature. At higher intensities, slower conducting fibers (1.0 – 8.0 m/s) were recruited, characteristic of Aδ fibers. Finally, at the highest intensities, very slow conducting fibers (<1.0 m/s) were recruited, characteristic of unmyelinated C fibers.

Recruitment profiles of T10 and L5 dorsal column stimulation

The results of afferents recruited by T10 and L5 stimulation are summarized in Table 2.

Stimulating at T10 recruited fiber populations with conduction velocities consistent with Aβ and Aδ afferents at room temperature in four out of four experiments (2.0-15.0 m/s). In one experiment, stimulation of T10 at 500 μA recruited an afferent population with a conduction velocity consistent with C fibers (0.28 m/s). While this conduction velocity is in the range of unmyelinated C fibers, it is more likely that this recruitment was just a very slow conducting population of Aδ afferents, due to the fact that most unmyelinated fibers are short system afferents, projecting only one or two spinal segments (Burgess & Horch, 1978). However, it is possible this is C fiber recruitment because some unmyelinated fibers may project more than five segments (Sugiura et al., 1989).

Stimulating at L5 was a level chosen because it is more likely to also recruit short system afferents originating from the L6 and S1 roots than T10 (Horch et al., 1976). Here, recruited fiber populations with conduction velocities were consistent with Aβ and Aδ afferents in four out of four experiments (4.0-20.0 m/s), and with C afferents in three out of four experiments (<1 m/s).

These findings support my neuroanatomical data showing presence of both myelinated and unmyelinated fibers in the dorsal column. Furthermore, the differing recruitment profiles between stimulation locations demonstrate the difference between short and intermediate/long system afferents in the dorsal column.

Dorsal column stimulation recruits calcium-dependent, synaptically mediated responses

In addition to the direct activation of primary afferents, stimulation of the dorsal column also recruited late arriving, spiking with inter-episode variability activity in dorsal roots, when superfusing physiologic levels of extracellular calcium with aCSF (2.4 mM Ca^{2+}) in the bath (Fig 6a-d). With low calcium aCSF (1.1 mM Ca^{2+}), this late, spiking activity is reversibly abolished (Fig 6e-h). Stimulation of both T10 and L5 recruited this activity in the L6 and S1 dorsal roots at stimulation intensities as low as 50 μA. These findings suggest that the late arriving, highly variable activity is due to calcium-dependent synaptic activation of interneurons with synapses on afferents (Jessell et al., 1986).

Discussion

Research into the potential uses of neuromodulation technologies is changing the field of medicine at a rapid and exciting pace. Nervous system modulating devices such as deep brain, spinal cord, and peripheral nerve stimulators are being increasingly used for a wide range of psychiatric and neurological disorders. High-jacking neural circuitry has proven to be a suitable alternative to pharmacological manipulation, as it is a more directed and cost-effective therapy, and is less likely to interfere with other medications (Kumar et al., 2002; Kumar et al., 2008).

While these devices have shown clinical efficacy, much of the basic science underlying these mechanisms is unknown. Success of *in vivo* animal studies has allowed for the advancement of translational studies that fail before they reach the clinic. This is likely due to an incomplete understanding at the basic level of how these stimulation devices are modulating neural circuitry. A better understanding of the anatomy and physiology of these circuits could potentially lead to more clinical success with current and future neuromodulatory devices.

Preclinical investigations and animal models have demonstrated the potential for using SCS for bladder dysfunction due to paralysis following SCI (Hong et al., 2008; Gad et al., 2014; Abud et al., 2015). An advancement of this kind would be significant for a number of reasons. First, bladder dysfunction is one of the major concerns patients with SCI would like alleviated (Anderson 2004). Second, the use of SCS in SCI patients for the treatment of chronic pain and paralysis is being researched and showing great potential (Kumar et al., 2007; Harkema et al., 2011).

If a patient is already receiving a SCS for one of these reasons, understanding its effect on the urinary system is a key consideration. Finally, SCS provides a more effective and less risky alternative to current stimulation methods to treat bladder dysfunction (Rijkhoff et al., 1997; Gad et al., 2014).

The findings presented in this study describe the basic anatomical and electrophysiological characteristics implicated in the use of SCS to modulate bladder circuitry. These findings support physiological studies suggesting that SCS modulates Aδ and C afferents of the dorsal column associated with sensory bladder information (Keast & De Groat, 1992; Hong et al., 2008). Many studies of this nature focus on just one aspect, either the anatomy or the physiology, and fail to merge the two concepts. By demonstrating the presence of both myelinated and unmyelinated fibers in the dorsal column alongside electrophysiological data demonstrating the recruitment of primary afferents, a clearer understanding of the basic anatomy and physiology underlying SCS for bladder dysfunction is established.

Future studies should attempt to bridge these basic findings with the *in vivo* animal models of SCS induced micturition. These studies should attempt to target specific afferent fiber populations, Aβ, Aδ, and/or C, to determine which fibers are modulated in SCS. If stimulation at lower intensities induces micturition, the fibers likely are Aβ and/or Aδ. If, however, stimulation at lower intensities does not induce micturition and stimulation at higher intensities does, the fibers likely implicated are C. Furthermore, future studies should investigate the functional role of the synaptic activity that is recruited. Perhaps a model using c-fos to determine which neurons are being activated following dorsal column stimulation will demonstrate

whether it is a synaptically mediated corticospinal tract pathway or dorsal horn interneurons producing the observed calcium-dependent activity.

While my project provides anatomical and electrophysiological data related to SCS modulation of bladder circuitry in mouse, there are several limitations to this study. First, the electrophysiology experiments were done in an *in vitro* mouse model, meaning that these findings may not translate to functional or clinical efficacy in future studies. While this set-up allows for elegant stimulation and recordings, the mouse spinal cord anatomy and physiology differs from the human spinal cord, especially *in vitro*. Another important consideration is temperature control. The experiments were performed at room temperature as opposed to physiologic temperature. While comparisons between conduction velocities at room and at physiologic temperature electrophysiology can be made (Pinto et al., 2008), characteristics of neurotransmission may be affected. Furthermore, the electrode used for stimulation was contacting the dorsal column, whereas clinical SCS electrodes apply stimulation epidurally. The *in vitro* stimulation preparation involved a monopolar, monophasic stimulation paradigm, whereas clinical SCS devices use arrays of 4-12 electrodes. A more relevant electrode set-up would require multiple electrodes to be raised approximately 200-500 μm above the cord. Finally, the neuroanatomical study only analyzes T10 of the dorsal column. This level does have significance in terms of clinical SCS, but analysis of cross sections from the lumbar and sacral regions, as well as images from the L6 and S1 roots, would lead to a better understanding of the neuroanatomy implicated in SCS modulation of bladder circuitry.

Conclusion

The characterization of the neuroanatomy of the mouse T10 dorsal column is consistent with imaging studies in other mammals. The dorsal column contains 0.1-0.3 μm unmyelinated fibers and 0.5-6.0 μm myelinated fibers. Different regions within the dorsal column contain differing proportions of the two fiber types.

Recordings from the L6 and S1 dorsal roots demonstrate that stimulation of the dorsal column at recruits Aβ, Aδ, and C afferents. Stimulation at T10 and L5 at low intensities recruits Aβ and Aδ fibers, and high intensity stimulation of L5 recruits C fibers. In addition to primary afferent activation, dorsal column stimulation recruits calcium-dependent synaptic activity.

References

Abud, Edsel M., Ronaldo M. Ichiyama, Leif A. Havton, and Huiyi H. Chang. "Spinal Stimulation of the Upper Lumbar Spinal Cord Modulates Urethral Sphincter Activity in Rats after Spinal Cord Injury." *American Journal of Physiology - Renal Physiology* 308.9 (2015): n. pag. Web.

Almeida, Tatiana F., Suely Roizenblatt, and Sergio Tufik. "Afferent Pain Pathways: A Neuroanatomical Review." *Brain Research* 1000.1-2 (2004): 40-56. Web.

Anderson, Kim D. "Targeting Recovery: Priorities of the Spinal Cord-Injured Population." *Journal of Neurotrauma* 21.10 (2004): 1371-383. Web.

Baba, H., M. Yoshimura, S. Nishi, and K. Shimoji. "Synaptic Responses of Substantia Gelatinosa Neurones to Dorsal Column Stimulation in Rat Spinal Cord in Vitro." *The Journal of Physiology* 478.1 (1994): 87-99. Web.

Birder, Lori A., James R. Roppolo, Vickie L. Erickson, and William C. De Groat. "Increased C-fos Expression in Spinal Lumbosacral Projection Neurons and Preganglionic Neurons after Irritation of the Lower Urinary Tract in the Rat." *Brain Research* 834.1-2 (1999): 55-65. Web.

Bors, E., and A.E. Comarr. "Chapter II Micturition." *Neurological Urology* (1971): 31-60. Web.

Boyce, W. H. "Electrical Stimulation of the Bladder." *BMJ* 1.5441 (1965): 1011-012. Web.

Braz, J., Carlos Solorzano, Xidao Wang, and A. Basbaum. "Transmitting Pain and Itch Messages: A Contemporary View of the Spinal Cord Circuits That Generate Gate Control." *Neuron* 82.3 (2014): 522-36. Web.

Burgess, P.r., and K.w. Horch. "The Distinction between the Short and Intermediate Ascending Pathways in the Fasciculus Gracilis of the Cat." *Brain Research* 151.3 (1978): 579-80. Web.

Cameron, Tracy. "Safety and Efficacy of Spinal Cord Stimulation for the Treatment of Chronic Pain: A 20-year Literature Review." *Journal of Neurology* 100 (2004): 254-67. Web.

Chung, Kyungsoon, Lauren A. Langford, Arnold E. Applebaum, and Richard E. Coggeshall. "Primary Afferent Fibers in the Tract of Lissauer in the Rat." *The Journal of Comparative Neurology* 184.3 (1979): 587-98. Web.

Dijkers, Marcel. "Prevalence of Chronic Pain after Traumatic Spinal Cord Injury: A Systematic Review." *Journal of Rehabilitation Research and Development* 46.1 (2009): 13-30. Web.

Fuentes, R., P. Petersson, W. B. Siesser, M. G. Caron, and M. A. L. Nicolelis. "Spinal Cord Stimulation Restores Locomotion in Animal Models of Parkinson's Disease." *Science* 323.5921 (2009): 1578-582. Web.

Gad, Parag N., Roland R. Roy, Hui Zhong, Daniel C. Lu, Yury P. Gerasimenko, and V. Reggie Edgerton. "Initiation of Bladder Voiding with Epidural Stimulation in Paralyzed, Step Trained Rats." *PLoS ONE* 9.9 (2014): n. pag. Web.

Gianino, Janet M., Judith A. Paice, and Michelle M. York. "Spinal Cord Anatomy." *Intrathecal Drug Therapy for Spasticity and Pain* (1996): 3-14. Web.

Glees, P., and J. Soler. "Fibre Content of the Posterior Column and Synaptic Connections of the Nucleus Gracilis." *Z. Zellforsch* 36 (1951): 381-400. Print.

Gulley, Robert L. "Golgi Studies of the Nucleus Gracilis in the Rat." *The Anatomical Record* 177.3 (1973): 325-42. Web.

Hand, Peter J. "Lumbosacral Dorsal Root Terminations in the Nucleus Gracilis of the Cat. Some Observations on Terminal Degeneration in Other Medullary Sensory Nuclei." *The Journal of Comparative Neurology* 126.2 (1966): 137-56. Web.

Harkema, Susan, Yury Gerasimenko, Jonathan Hodes, Joel Burdick, Claudia Angeli, Yangsheng Chen, Christie Ferreira, Andrea Willhite, Enrico Rejc, Robert G. Grossman, and V. Reggie Edgerton. "Effect of Epidural Stimulation of the Lumbosacral Spinal Cord on Voluntary Movement, Standing, and Assisted Stepping after Motor Complete Paraplegia: A Case Study." *The Lancet* 377.9781 (2011): 1938-947. Web.

Harper, A. A., and S. N. Lawson. "Conduction Velocity Is Related to Morphological Cell Type in Rat Dorsal Root Ganglion Neurones." *The Journal of Physiology* 359.1 (1985): 31-46. Web.

Holsheimer, Jan. "Computer Modelling of Spinal Cord Stimulation and Its Contribution to Therapeutic Efficacy." *Spinal Cord* 36.8 (1998): 531-40. Web.

Hong, Chang Hee, Hye-Young Lee, Mei Hua Jin, Ji Yeun Noh, Bong Hee Lee, and Sang Won Han. "The Effect of Intravesical Electrical Stimulation on Bladder Function and Synaptic Neurotransmission in the Rat Spinal Cord after Spinal Cord Injury." *BJU International* 103.8 (2009): 1136-141. Web.

Horch, K., P. Burgess, and D. Whitehorn. "Ascending Collaterals of Cutaneous Neurons in the Fasciculus Gracilis of the Cat." *Brain Research* 117.1 (1976): 1-17. Web.

Hursh, J. B. "Conduction Velocity and Diameter of Nerve Fibers." *American Journal of Physiology* 127 (1939): 131-39. Print.

Janssen, Dick A. W., Joost G. Hoenderop, John P. F. A. Heesakkers, and Jack A. Schalken. "TRPV4 Mediates Afferent Pathways in the Urinary Bladder. A Spinal C-fos Study Showing TRPV1 Related Adaptations in the TRPV4 Knockout Mouse." *European Journal of Physiology* 468.10 (2016): 1741-749. Web.

Jessell, T. M., K. Yoshioka, and C. E. Jahr. "Amino Acid Receptor-Mediated Transmission at Primary Afferent Synapses in Rat Spinal Cord." *J. Exp. Biol.* 124 (1986): 239-58. Web.

Jiang, Zhiyu, Kevin P. Carlin, and Robert M. Brownstone. "An in Vitro Functionally Mature Mouse Spinal Cord Preparation for the Study of Spinal Motor Networks." *Brain Research* 816.2 (1999): 493-99. Web.

Keast, J. R., and W. C. De Groat. "Segmental Distribution and Peptide Content of Primary Afferent Neurons Innervating the Urogenital Organs and Colon of Male Rats." *The Journal of Comparative Neurology* 319.4 (1992): 615-23. Web.

Kumar, Krishna, Rod S. Taylor, Line Jacques, Sam Eldabe, Mario Meglio, Joan Molet, Simon Thomson, Jim O'callaghan, Elon Eisenberg, Germain Milbouw, Eric Buchser, Gianpaolo Fortini, Jonathan Richardson, and Richard B. North. "The Effects of Spinal Cord Stimulation in Neuropathic Pain Are Sustained: A 24-month Follow-up of the Prospective Randomized Controlled Multicenter Trial of the Effectiveness of Spinal Cord Stimulation." *Neurosurgery* 63.4 (2008): 762-70. Web.

Kumar, Krishna, Rod S. Taylor, Line Jacques, Sam Eldabe, Mario Meglio, Joan Molet, Simon Thomson, Jim Callaghan, Elon Eisenberg, Germain Milbouw, Eric Buchser, Gianpaolo Fortini, Jonathan Richardson, and Richard B. North. "Spinal Cord Stimulation versus Conventional Medical Management for Neuropathic Pain: A Multicentre Randomised Controlled Trial in Patients with Failed Back Surgery Syndrome." *Pain* 132.1 (2007): 179-88. Web.

Kumar, Krishna, Samaad Malik, and Denny Demeria. "Treatment of Chronic Pain with Spinal Cord Stimulation versus Alternative Therapies: Cost-effectiveness Analysis." *Neurosurgery* 51.1 (2002): 106-16. Web.

Madersbacher, H. "The Various Types of Neurogenic Bladder Dysfunction: An Update of Current Therapeutic Concepts." *Paraplegia* 28.4 (1990): 217-29. Web.

Mcneill, D. L., K. Chung, S. M. Carlton, and R. E. Coggeshall. "Calcitonin Gene-related Peptide Immunostained Axons Provide Evidence for Fine Primary Afferent Fibers in the Dorsal and Dorsolateral Funiculi of the Rat Spinal Cord." *The Journal of Comparative Neurology* 272.2 (1988): 303-08. Web.

Mcneill, Daniel L., Richard E. Coggeshall, and Susan M. Carlton. "A Light and Electron Microscopic Study of Calcitonin Gener-related Peptide in the Spinal Cord of the Rat." *Experimental Neurology* 99.3 (1988): 699-708. Web.

Meglio, M., B. Cioni, E. D'amico, G. Ronzoni, and G. F. Rossi. "Epidural Spinal Cord Stimulation for the Treatment of Neurogenic Bladder." *Acta Neurochirurgica* 54.3-4 (1980): 191-99. Web.

Melzack, R., and P. D. Wall. "Pain Mechanisms: A New Theory." *Science* 150.3699 (1965): 971-78. Web.

National Spinal Cord Injury Statistical Center. "Spinal Cord Injury (SCI) Facts and Figures at a Glance." *The Journal of Spinal Cord Medicine* 39.1 (2016): 123-24. Web.

North, R. B., D. H. Kidd, M. Zahurak, C. S. James, and D. M. Long. "Spinal Cord Stimulation for Chronic, Intractable Pain." *Survey of Anesthesiology* 38.03 (1994): 162. Web.

Okamoto, M., H. Baba, P. A. Goldstein, H. Higashi, K. Shimoji, and M. Yoshimura. "Functional Reorganization of Sensory Pathways in the Rat Spinal Dorsal Horn following Peripheral Nerve Injury." *The Journal of Physiology* 532.1 (2001): 241-50. Web.

Ong, Henry H., and Felix W. Wehrli. "Quantifying Axon Diameter and Intra-cellular Volume Fraction in Excised Mouse Spinal Cord with Q-space Imaging." *NeuroImage* 51.4 (2010): 1360-366. Web.

Pinto, V., V. A. Derkach, and B. V. Safronov. "Role of TTX-Sensitive and TTX-Resistant Sodium Channels in AÂ - and C-Fiber Conduction and Synaptic Transmission." *Journal of Neurophysiology* 99.2 (2008): 617-28. Web.

Qi, Hui-Xin, and Jon H. Kaas. "Organization of Primary Afferent Projections to the Gracile Nucleus of the Dorsal Column System of Primates." *The Journal of Comparative Neurology* 499.2 (2006): 183-217. Web.

Rexed, Bror. "A Cytoarchitectonic Atlas of the Spinal Coed in the Cat." *The Journal of Comparative Neurology* 100.2 (1954): 297-379. Web.

Rijkhoff, N.j.m., H. Wijkstra, P.e.v. Van Kerrebroeck, and F.m.j. Debruyne. "Selective Detrusor Activation By Electrical Sacral Nerve Root Stimulation in Spinal Cord Injury." *The Journal of Urology* 157.4 (1997): 1504-508. Web.

Shealy, C. Norman, J. Thomas Mortimer, and James B. Reswick. "Electrical Inhibition of Pain by Stimulation of the Dorsal Columns." *Anesthesia & Analgesia* 46.4 (1967): n. pag. Web.

Shimizu, T., M. Yoshimura, H. Baba, K. Shimoji, and H. Higashi. "Role of A Delta Afferent Fibers in Modulation of Primary Afferent Input to the Adult Rat Spinal Cord." *Brain Research* 691.1-2 (1995): 92-98. Web.

Shreckengost, J., J. Calvo, J. Quevedo, and S. Hochman. "Bicuculline-Sensitive Primary Afferent Depolarization Remains after Greatly Restricting Synaptic Transmission in the Mammalian Spinal Cord." *Journal of Neuroscience* 30.15 (2010): 5283-288. Web.

Sugiura, Y., N. Terui, Y. Hosoya, and K. Kohno. "Distribution of Unmyelinated Primary Afferent Fibers in the Dorsal Horn." *Processing of Sensory Information in the Superficial Dorsal Horn of the Spinal Cord* (1989): 15-27. Web.

Vejsada, Richard, J. Paleak, Pavel H, and T. Soukup. "Postnatal Development of Conduction Velocity and Fibre Size in the Rat Tibial Nerve." *International Journal of Developmental Neuroscience* 3.5 (1985): 583-95. Web.

Watson, Charles, and Megan Harrison. "The Location of the Major Ascending and Descending Spinal Cord Tracts in All Spinal Cord Segments in the Mouse: Actual and Extrapolated." *The Anatomical Record: Advances in Integrative Anatomy and Evolutionary Biology* 295.10 (2012): 1692-697. Web.

Wheeler, Anthony H. "Spinal Cord Stimulation Technique: Approach Considerations, Device Summary, Percutaneous Trial of SCS Placement." *Spinal Cord Stimulation Technique: Approach Considerations, Device Summary, Percutaneous Trial of SCS Placement*. Medscape, 06 Jan. 2017. Web. 30 Mar. 2017.

Willis, William D., and Richard E. Coggeshall. *Sensory Mechanisms of the Spinal Cord*. New York: Kluwer Acad./Plenum, 2004. Print.

Fiber	Myelin?	Mean Axon Diameter	Peripheral Conduction Velocity
Aβ	Yes	>10 μm (Almeida et al., 2004)	9.4 – 26.7 m/s (Pinto et al, 2008)
Aδ	Yes	1.0 – 6.0 μm (Almeida et al., 2004)	1.1 – 9.4 m/s (Pinto et al., 2008)
C	No	0.4 – 1.2 μm (Almeida et al., 2004)	0.23 – 0.7 m/s (Pinto et al., 2008)

Table 1. Classification of dorsal column primary afferents. Imagining and electrophysiological studies in the dorsal column have laid the groundwork for identifying fiber populations based on their myelination, axon diameter, and conduction velocity. The conduction velocity data are taken in rat neurons at room temperature (Pinto et al., 2008).

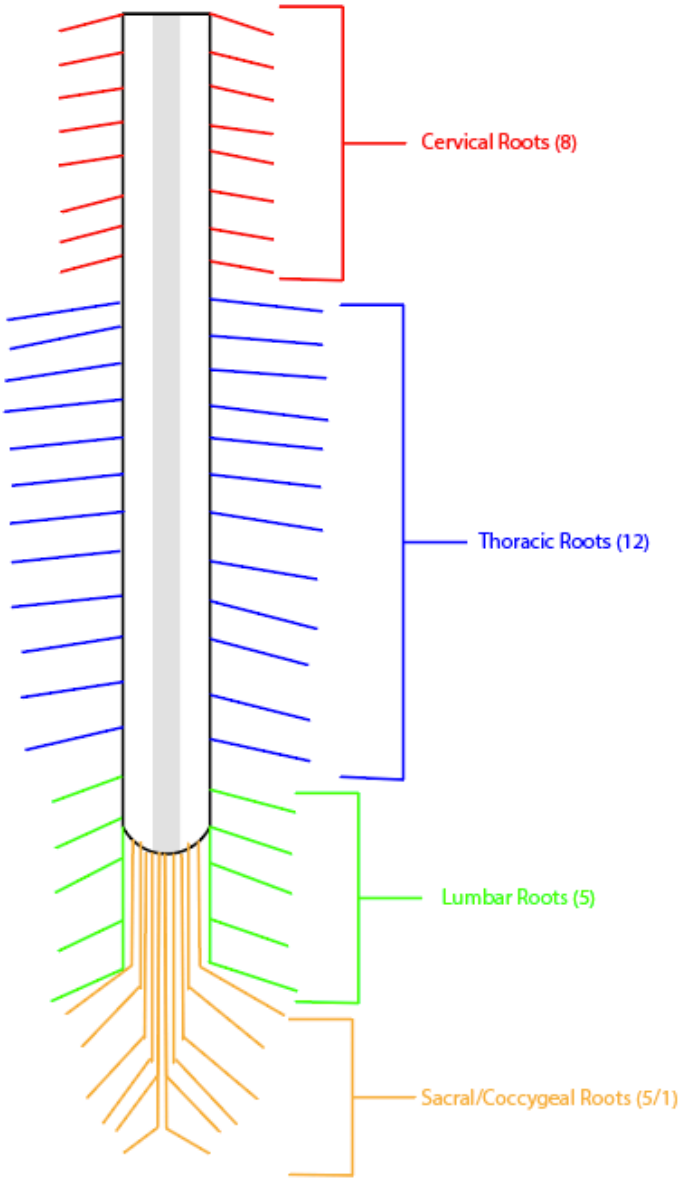

Fig 1. Anatomy of the dorsal spinal cord. The human spinal cord contains 31 pairs of dorsal roots: 8 cervical, 12 thoracic, 5 lumbar, 5 sacral, and 1 pair coccygeal roots. The spinal cord is encased in the vertebral column and extends caudal from the brain stem to approximately the L2 vertebrae. The dorsal column is represented by the grey shaded column in the medial region of the dorsal spinal cord. Primary afferents enter the spinal cord through dorsal roots and some ascend in the dorsal column. Short system neurons project 1 or 2 levels before terminating, intermediate system neurons project 4-12 levels, and long system neurons ascend all the way to the dorsal column nuclei of the medulla.

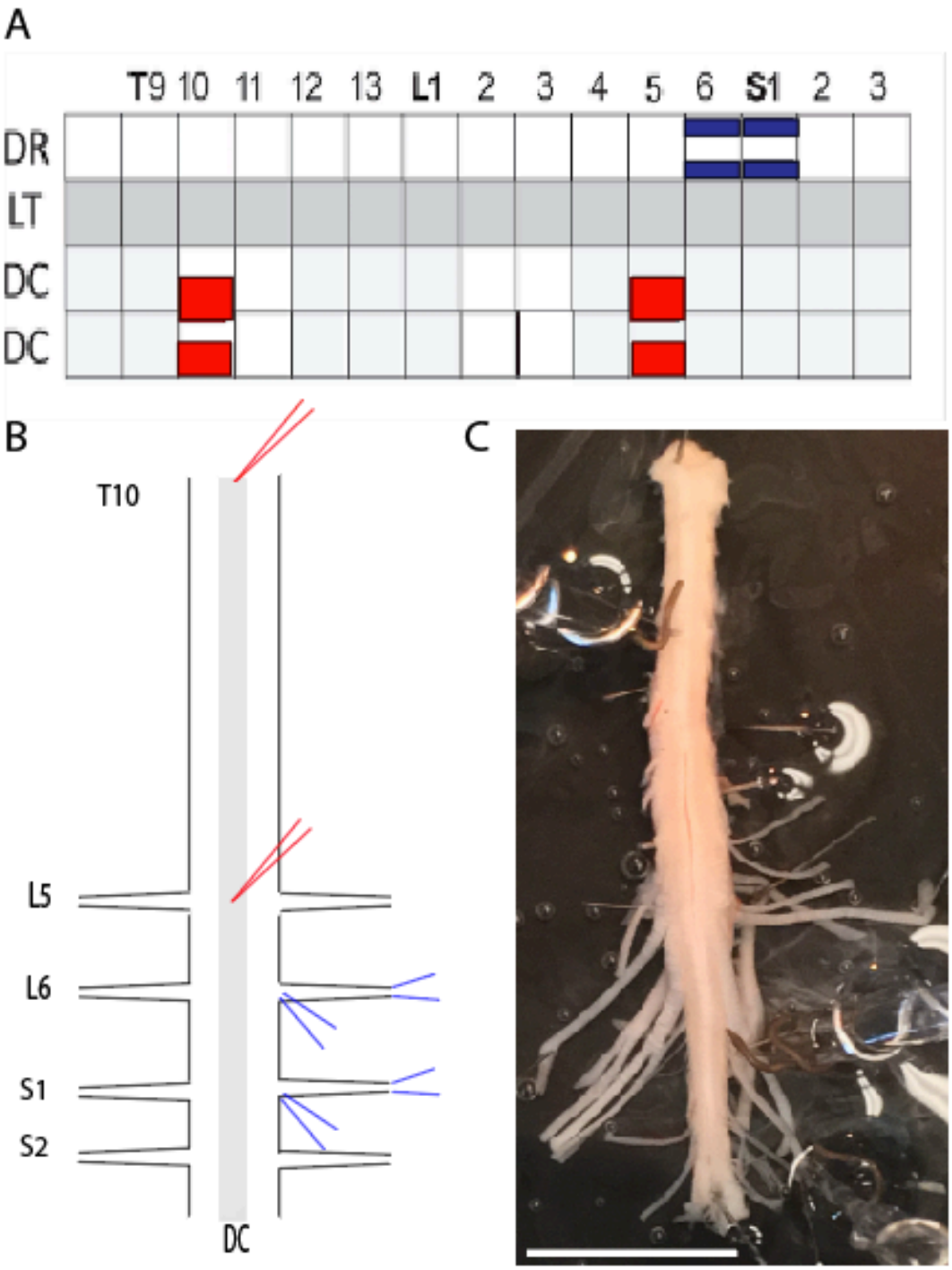

Fig 2. Electrophysiology protocol. A) Schematic of the stimulation and recording locations during the electrophysiology experiments. Red boxes indicate placement of the stimulating electrodes on the midline of T10 and L5 dorsal column. Blue boxes indicate the placement of recording electrodes on the L6 and S1 dorsal roots. B) Diagram displaying the electrode placement. The red electrodes show the two

locations of stimulation. The blue electrodes show the distal and proximal root recording locations. C) Photo of a typical experimental set up. The rostral electrode is stimulating T10 of the dorsal column and the two caudal electrodes are recording from the L6 dorsal root. Scale bar = 6 mm.

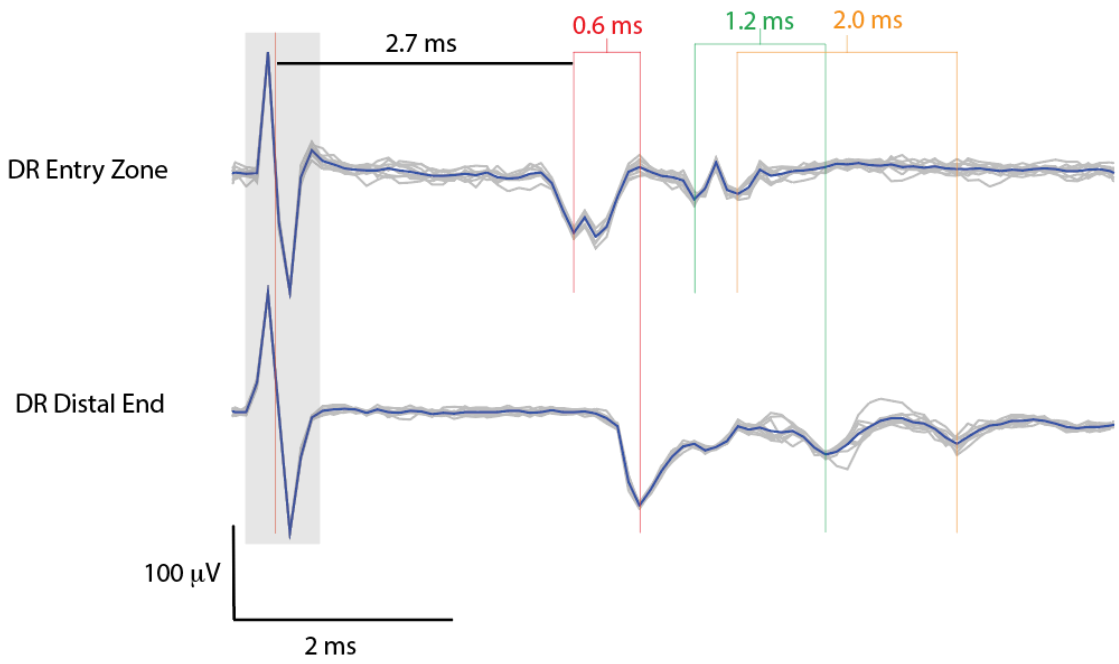

Fig 3. Determination of central and peripheral conduction velocities. In this experiment, the distance between the dorsal column (DC) stimulating electrode and the dorsal root (DR) proximal region was 12.0 mm and the distance between recording electrodes at the DR proximal region and distal end was 4.0 mm. Central conduction velocity was determined by dividing the distance between the DC stimulating electrode and the DR proximal region recording site by the time between the stimulus pulse offset and the peak of the first arriving volley. Peak to peak analysis was selected because it is a more consistent measure of compound action potential velocity than initiation. For this trace, the signal traveled 12.0 mm in 2.7 ms, giving a conduction velocity of 4.44 m/s. Peripheral conduction velocity was determined by dividing the distance between the DR proximal region and distal end recording sites by the time between corresponding volleys. For this trace, three compound action potential volleys were recorded by both electrodes, with time differences of 0.6 ms (red vertical bars), 1.2 ms (green vertical bars), and 2.0 ms (orange vertical bars, giving conduction velocities of 6.7 m/s, 3.3 m/s, and 2.0 m/s. The stimulus intensity used was 50 μA for 200 μs at medial T10 and the recordings are from the L6 dorsal root.

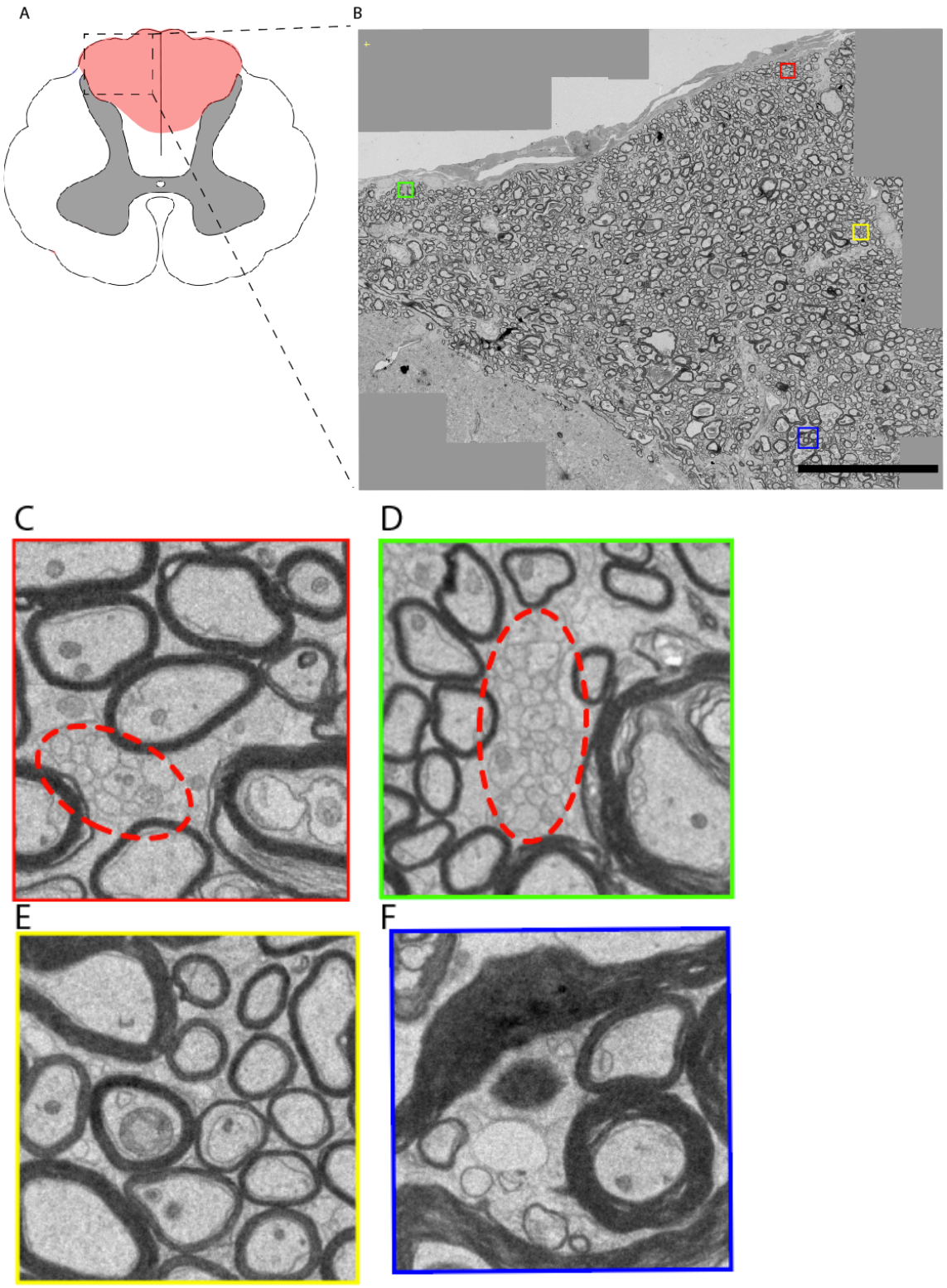

Fig 4. Electron micrograph analysis of T10 dorsal column axons. A) Cross-section of the spinal cord with the dorsal column shaded red. All images analyzed were taken from this region. B) Magnified image of the adult mouse T10 dorsal

column. This image contains mostly dorsal column axons with a small portion of the dorsal horn located in the bottom left corner. Scale bar = 50 μm. C-F) 16000x magnified images of populations of myelinated and unmyelinated axons. Each box is 5.13 x 5.13 μm. In C and D, the unmyelinated populations are encircled by red dotted lines. C) Region near the surface of the spinal cord containing both myelinated and unmyelinated axons. D) Lateral region near the surface of the spinal cord containing both myelinated and unmyelinated axons. E) High density population of myelinated axons in the medial region of the dorsal column. F) This image demonstrates the wide range of myelin thickness present in the dorsal column.

A

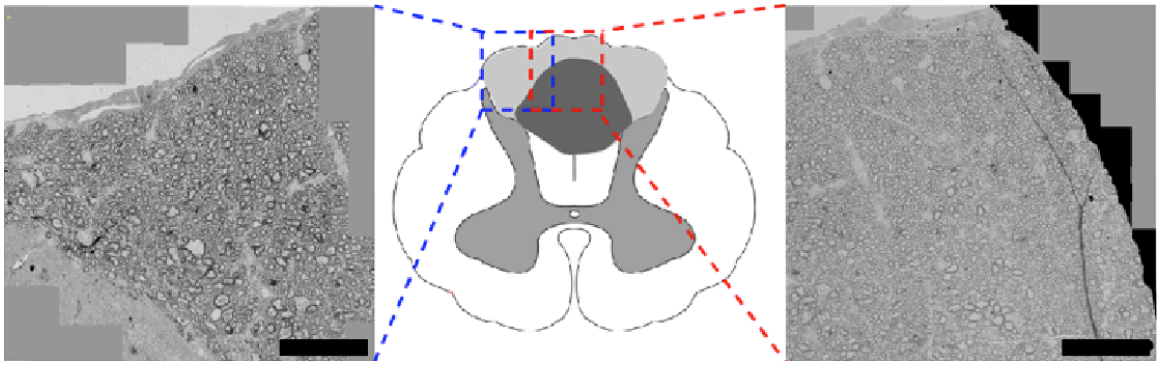

B

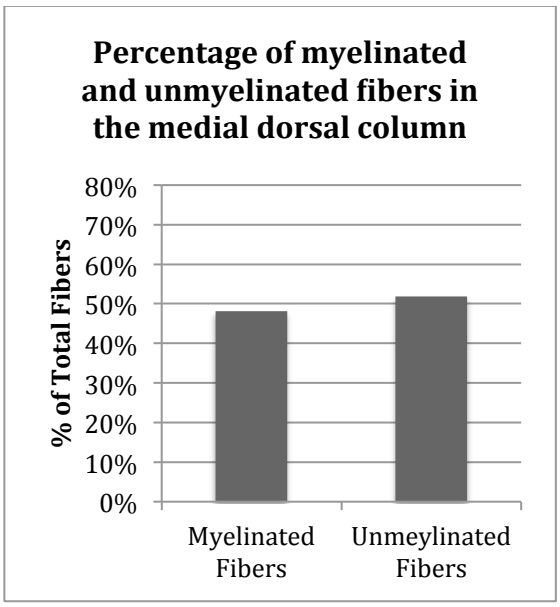
Percentage of myelinated and unmyelinated fibers in the medial dorsal column
% of Total Fibers
80%
70%
60%
50%
40%
30%
20%
10%
0%
Myelinated Fibers
Unmeylinated Fibers

C

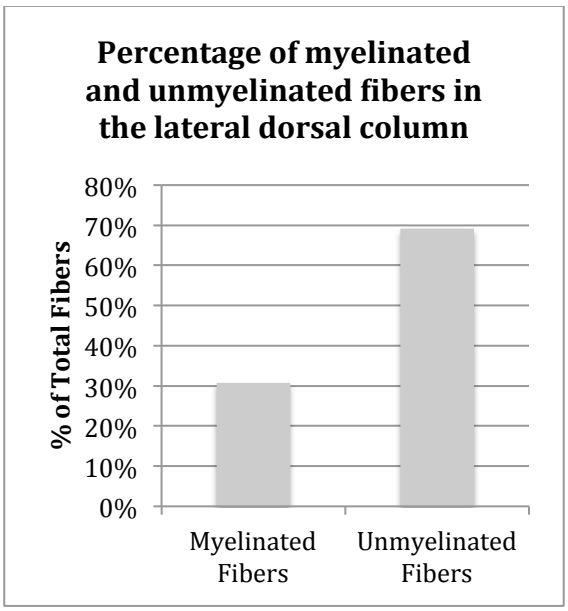
Percentage of myelinated and unmyelinated fibers in the lateral dorsal column
% of Total Fibers
80%
70%
60%
50%
40%
30%
20%
10%
0%
Myelinated Fibers
Unmyelinated Fibers

D

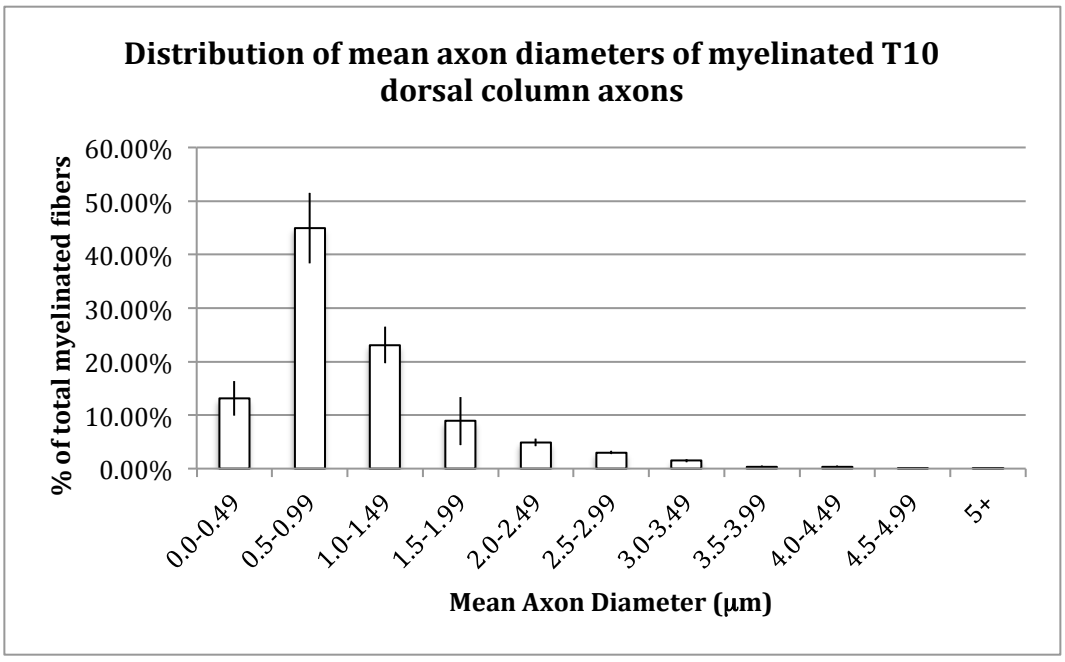
Distribution of mean axon diameters of myelinated T10 dorsal column axons
% of total myelinated fibers
60.00%
50.00%
40.00%
30.00%
20.00%
10.00%
0.00%
0.0-0.49
0.5-0.99
1.0-1.49
1.5-1.99
2.0-2.49
2.5-2.99
3.0-3.49
3.5-3.99
4.0-4.49
4.5-4.99
5+
Mean Axon Diameter (μm)

Fig 5. Characteristics of axon populations in the adult mouse T10 dorsal column. A) Two low magnification images taken from one animal. The diagram in the middle shows the differentiation between the medial (dark gray region) and lateral (light grey) regions of the dorsal column. The image on the left shows axons from both the medial and lateral regions, as well as a small part of the dorsal horn. The image on the right shows axons mostly from the medial region. Scale bars = 50 μm B) In the more medial regions, the number of myelinated and unmyelinated fibers were approximately equal (7355 myelinated; 7911 unmyelinated; n=1) C) In the more lateral regions, there were a little over twice as many unmyelinated than myelinated fibers (5712 myelinated;12821 unmyelinated; n=1). D) The distribution of mean axon diameters of myelinated axons in the dorsal column (n=2). Error bars represent standard deviation.

Intensity	STIM – REC	Aβ (>10 m/s)	Aδ (1-10 m/s)	C (< 1 m/s)
50 μA	T10 – L6	3/4	3/4	0/4
	T10 – S1	4/4	4/4	0/4
	L5 – L6	3/4	3/4	0/4
	L5 – S1	4/4	4/4	0/4
200 μA	T10 – L6	3/4	3/4	0/4
	T10 – S1	4/4	4/4	0/4
	L5 – L6	3/4	3/4	1/4
	L5 – S1	4/4	4/4	2/4
500 μA	T10 – L6	3/4	3/4	0/4
	T10 – S1	4/4	4/4	1/4
	L5 – L6	3/4	3/4	3/4
	L5 – S1	4/4	4/4	2/4

Table 2. Afferent fiber recruitment in L6 and S1 dorsal roots during medial T10 and L5 dorsal column stimulation. Four electrophysiology experiments were performed stimulating both the T10 and L5 medial region of the dorsal column at intensities of 50, 200, and 500 μA for 200 μs, recording from the L6 and S1 dorsal roots. While 50 and 200 μA pulses are clinically relevant, 500 μA are not and may in fact damage spinal tissue. The fractions represent the number of experiments that successfully recruited the given afferent population. Fiber populations with conduction velocities consistent with Aβ and Aδ afferents were recruited at all intensities in almost every experiment. Fiber populations with conduction velocities consistent with C fibers were recruited with L5 stimulation with higher intensities of 200 and 500 μA. T10 stimulation recruited this very slow conducting population in one experiment with the highest intensity stimulation.

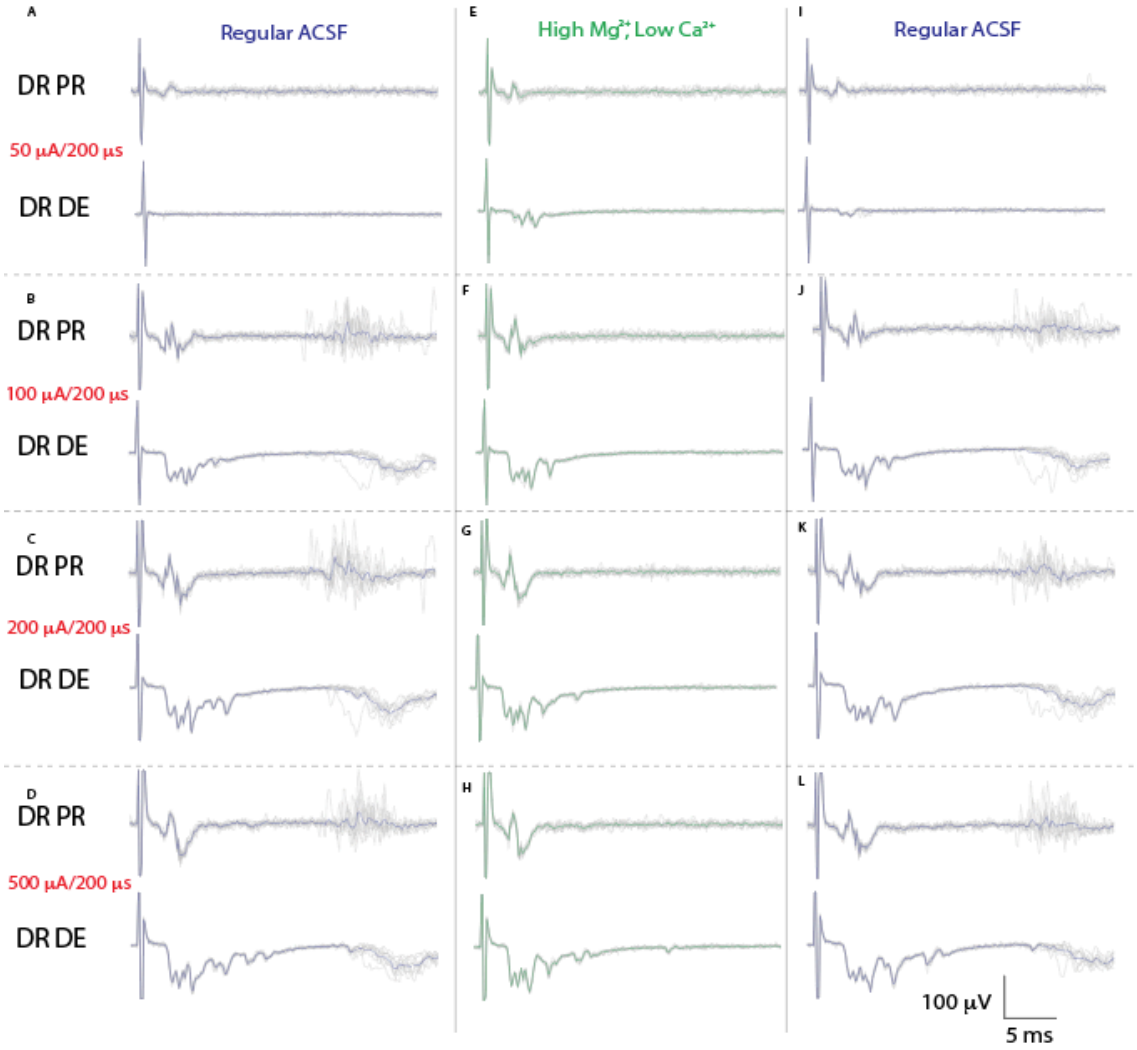

Fig 6. Stimulations in high and low calcium demonstrate the presence of calcium-dependent, synaptically evoked activity. The left panels (A-D) show recordings from the L6 dorsal root (DR) proximal region (PR) and distal end (DE) during medial T10 stimulation at increasing intensities in aCSF with calcium show late arriving, highly variable activity. The middle panels (E-H) show recordings during medial T10 stimulation in low calcium aCSF. In the absence of calcium, this late arriving, highly variable activity disappears. When calcium is returned to the set-up (I-L), the activity returns.